International Nano Letters
a SpringerOpen Journal

ORIGINAL ARTICLE Open Access

Influence of Zn^{2+} doping on the structural and surface morphological properties of nanocrystalline Ni-Cu spinel ferrite

Vidyadhar V Awati[1], Sopan M Rathod[2], Maheshkumar L Mane[3*] and Kakasaheb C Mohite[4]

Abstract

$Ni_{0.8-x}Cu_{0.2}Zn_xFe_2O_4$ ($x = 0.0 \leq 0.6$ with steps of 0.2) ferrite nanophase was achieved by sol–gel auto-combustion technique. The as-prepared samples were thermally characterized by thermogravimetry/differential thermal analysis to obtain firing temperature of the materials. The X-ray diffraction pattern indicates the formation of a single-phase cubic spinel structure and shows strong influence of the incorporation of Zn^{2+} metal ions on the spinel structure. The annealing treatment does not alter the crystal structure but increases the crystallinity of the samples. The morphological investigations and nanometric sizes of the samples were studied by scanning electron microscopy and transmission electron microscopy. The crystallographic texture due to annealing and Zn^{2+} ion doping was systematically investigated by Fourier transform infrared spectroscopy.

Keywords: Ferrite, Crystal structure, Annealing treatment, Morphology
PACS: 75.50.Gg, 74.25.Ld, 43.35.Cg

Background

The development of civilization has been intimately linked with the ability of human beings to work with advanced magnetic nanomaterials. Nanocrystalline magnetic particles with specific properties can be synthesized by different chemical techniques [1-4]. These properties are strongly dependent on their shape, size, crystallinity, and distribution of the cations among the tetrahedral (A) and octahedral (B) sites of the spinel structure. The use of nanoparticles for desired applications has attracted considerable attention in recent years because nanoparticles provide high surface area-to-volume ratios [5,6]. Magnetic particles are gaining attraction due to a variety of technological applications such as high-density information storage nanodevices, ferrofluids, magnetic refrigeration, residential cooling, and biomedical applications like magnetic separations, biosensors, resonance imaging, hyperthermia, and targeted and controlled drug delivery. In this regard, spinel ferrites are particularly important because of their excellent magnetic properties that can be tuned to suit the requirement using chemical manipulations [7-11]. However, the development of novel techniques for improvements of the magnetic and the structural properties of soft magnetic spinel ferrites has been the objective of numerous studies in past decades.

Recently, Ni-Cu-Zn spinel ferrites with nanometric dimensions were extensively studied in order to develop multilayer chip inductors [12-15]. Many methods such as sol–gel auto-combustion technique [16], chemical coprecipitation [17], citrate precursor method [18], oxalate precursor technique [19], and ceramic method [20] are used to prepare Ni-Cu-Zn spinel ferrite. Among them, the sol–gel auto-combustion method has unique advantages such as excellent composition control, low temperature process, low production cost, and better results.

In the present investigation, we report the sol–gel auto-combustion synthesis of Ni-Cu-Zn ferrite. The Ni-Cu spinel ferrite material allows the introduction of Zn^{2+} cation in the spinel matrix, which causes the change in the structure and surface morphology considerably. Optimization of Zn^{2+} concentration with respect to Ni^{2+} will be investigated. Correlation between compositions of Ni-Cu-Zn spinel ferrites and sintering temperatures on

* Correspondence: mane.maheshkumar@hotmail.com
[3]Department of Physics, S.G.R.G. Shinde Mahavidyalaya, Paranda 413502 (MS), India
Full list of author information is available at the end of the article

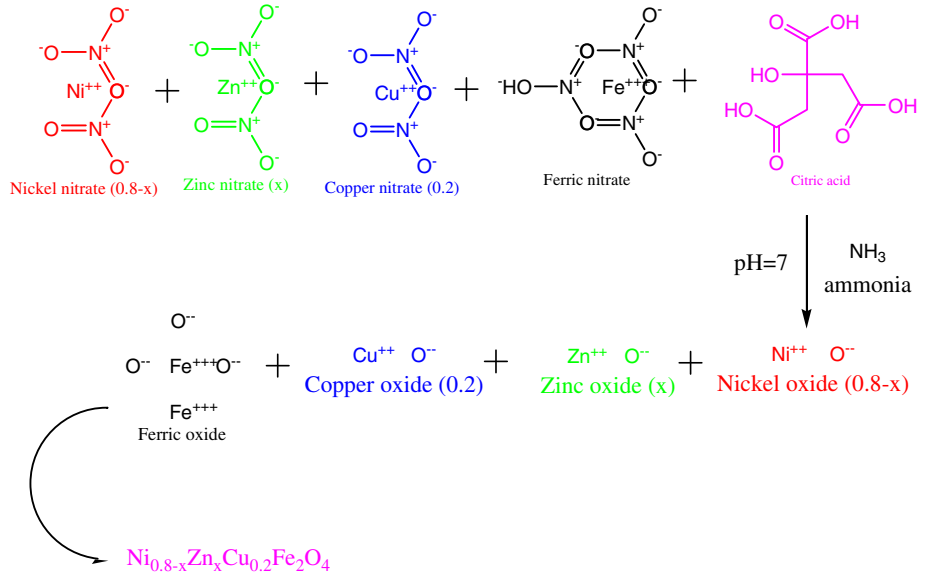

Figure 1 Chemical reaction of $Ni_{0.8-x}Zn_xCu_{0.2}Fe_2O_4$.

structural, infrared, and morphological behaviors has been carried out.

Methods

A spinel ferrite compositions of $Ni_{0.8-x}Zn_xCu_{0.2}Fe_2O_4$ (with x = 0.0, 0.2, 0.4, and 0.6) nanoparticles were prepared using the sol–gel auto-combustion technique from the high-purity analytical grade solutions of $Fe(NO_3)_3{\cdot}9H_2O$, $Cu(NO_3)_2{\cdot}3H_2O$, $Zn(NO_3)_2{\cdot}6H_2O$, and $Ni(NO_3)_2{\cdot}6H_2O$. Citric acid was used as fuel. The weighed amounts of these salts were completely dissolved in distilled water, and the solution was stirred for half an hour. This solution was then added to citric acid in such a way that in the final sample, the molar ratio of these nitrates and citric acid becomes 1:3. A small amount of ammonia was simultaneously added drop-wise to maintain the pH of 7 with continuous stirring of the solution. The as-prepared spinel ferrite materials were annealed at 400°C and 700°C for 2 h after confirmation by thermogravimetry (TG)-differential thermal analyses (DTA). The schematic of the chemical reaction

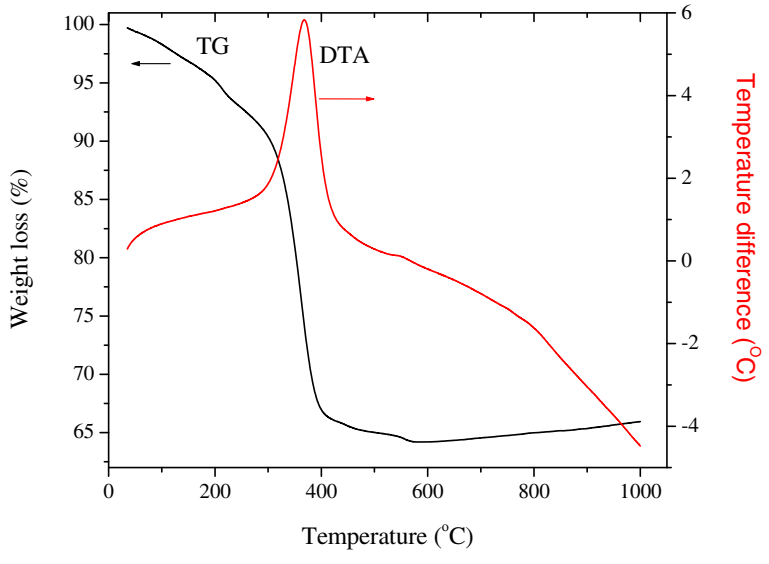

Figure 2 TG/DTA plot for typical sample at x = 0.4.

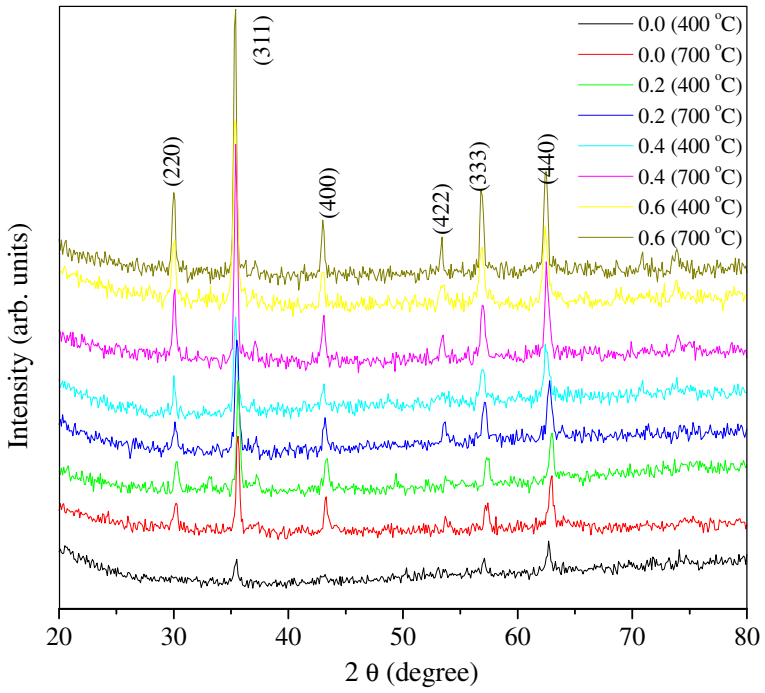

Figure 3 X-ray diffraction patterns of $Ni_{0.8-x}Zn_xCu_{0.2}Fe_2O_4$($x$ = 0.0, 0.2, 0.4, and 0.6).

involved in the present investigated ferrite system is depicted in Figure 1. The general nitrate-citrate combustion reaction may be written as follows:

$$(0.8-x)\mathrm{Ni(NO_3)_2{\cdot}6H_2O} + 0.2\mathrm{Cu(NO_3)_2{\cdot}3H_2O} + x\mathrm{Zn(NO_3)_2{\cdot}6H_2O} + 2\mathrm{Fe(NO_3)_3{\cdot}9H_2O} + 3\mathrm{C_6H_8O_7} \rightarrow (\mathrm{Ni_{0.8-x}Cu_{0.2}Zn_xFe_2O_4}) + 4\mathrm{N_2}\uparrow + 18\ \mathrm{CO_2}\uparrow + 36\mathrm{H_2O}\uparrow.$$

The thermal behavior analysis of the as-prepared sample was carried out on a PerkinElmer system (model Diamond TG/DTA, PerkinElmer, Waltham, MA, USA) under air atmosphere in the temperature range from ambient to 1,000°C. The phase identification and structure analysis of the thermally treated powders were carried out by X-ray diffraction (XRD) analysis using a Philips X-ray diffractometer (model PW 3710, Philips, Amsterdam, The Netherlands). The morphological studies were carried out by field-emission gun scanning electron microscopy using JSM-7600F with an accelerating voltage of 0.1 to 30 kV and transmission electron microscopy (TEM) using Philips (model CM200) operating at 20 to 200 kV with a resolution of 2.4 Å. The Fourier transform infrared (FTIR) spectroscopy (model MAGNA 550, Nicolet Instruments Corporation, Madison, WI, USA)was taken in the range of 400 to 4,000 cm^{-1}.

Table 1 Variation of lattice constant and crystallite size of $Ni_{0.8-x}Zn_xCu_{0.2}Fe_2O_4$ annealed at 400°C and 700°C

Zn^{2+}content	Lattice constant (Å)		Crystallite site (nm)	
	400°C	700°C	400°C	700°C
0.0	8.334	8.351	100.854	124.627
0.2	8.360	8.374	131.258	159.579
0.4	8.386	8.394	163.687	177.400
0.6	8.407	8.426	181.642	219.498

Results and discussion

In order to investigate the thermal growth process of $Ni_{0.8-x}Zn_xCu_{0.2}Fe_2O_4$ nanoparticles, TG-DTA of the as-prepared powder samples were carried out from 30°C to 1,000°C. The typical TG-DTA curve for the sample x = 0.4 is shown in Figure 2. From TGA, a total weight loss of approximately 35% was observed when the sample was heated between ambient to 1,000°C in air. A weight loss of approximately 10% occurred between 30°C to 300°C that could be assigned to the elimination of surface water and solvents that remained in the material even after drying. The major weight loss at 300°C to 400°C attributed to the loss of structural water and the decomposition of organic compounds and nitrates. As expected, the decomposition reaction is strongly exothermic. In the DTA curve, we can observe that an exothermic peakat 370°C associated withthe decomposition of organic compounds in the structure due to the crystallization of the spinel ferrite material is relatively

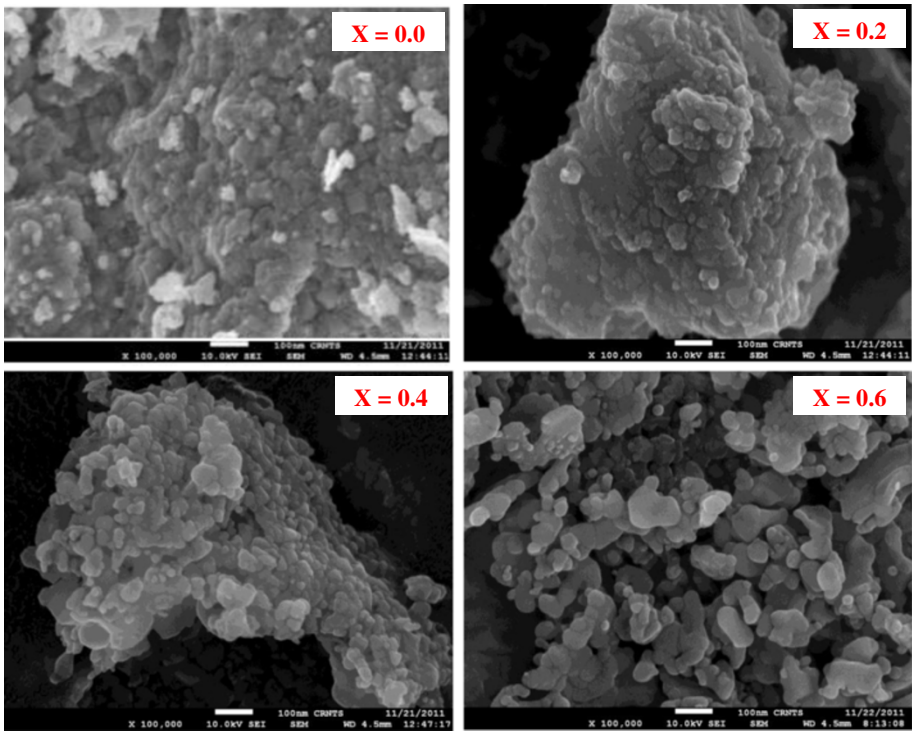

Figure 4 Scanning electron microscopy images of $Ni_{0.8-x}Zn_xCu_{0.2}Fe_2O_4$ (annealed at 400°C).

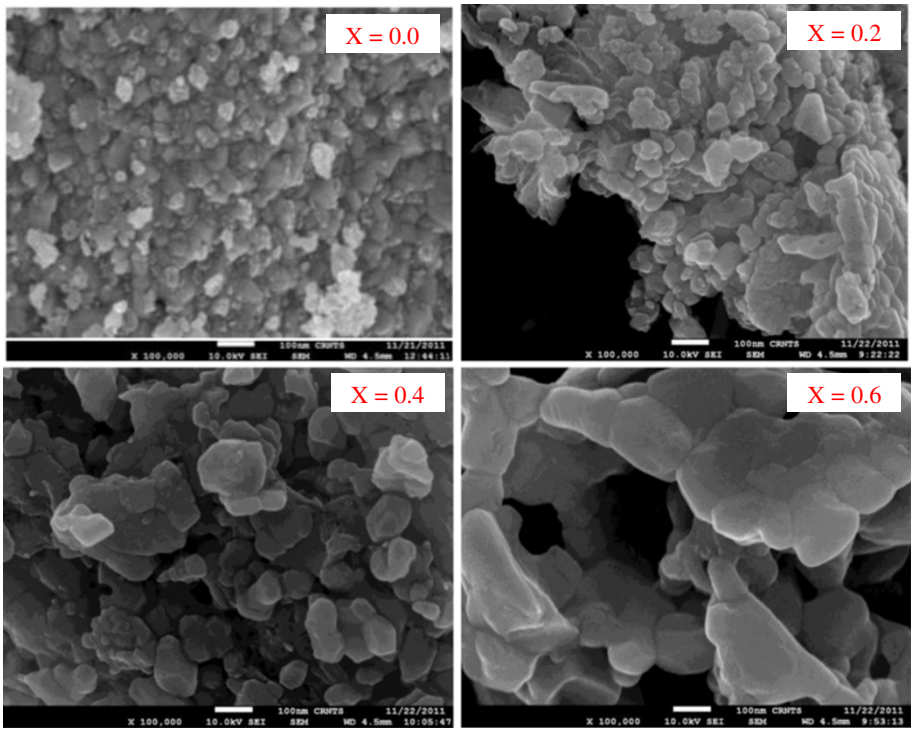

Figure 5 Scanning electron microscopy images of $Ni_{0.8-x}Zn_xCu_{0.2}Fe_2O_4$ (annealed at 700°C).

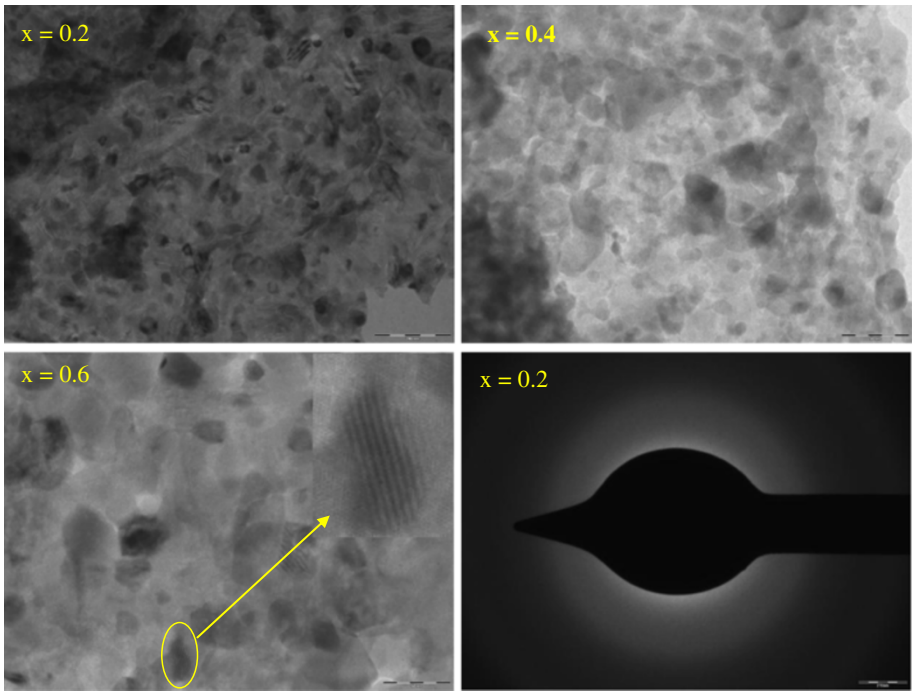

Figure 6 Transmission electron microscopy images of $Ni_{0.6}Zn_{0.2}Cu_{0.2}Fe_2O_4$ (as burnt).

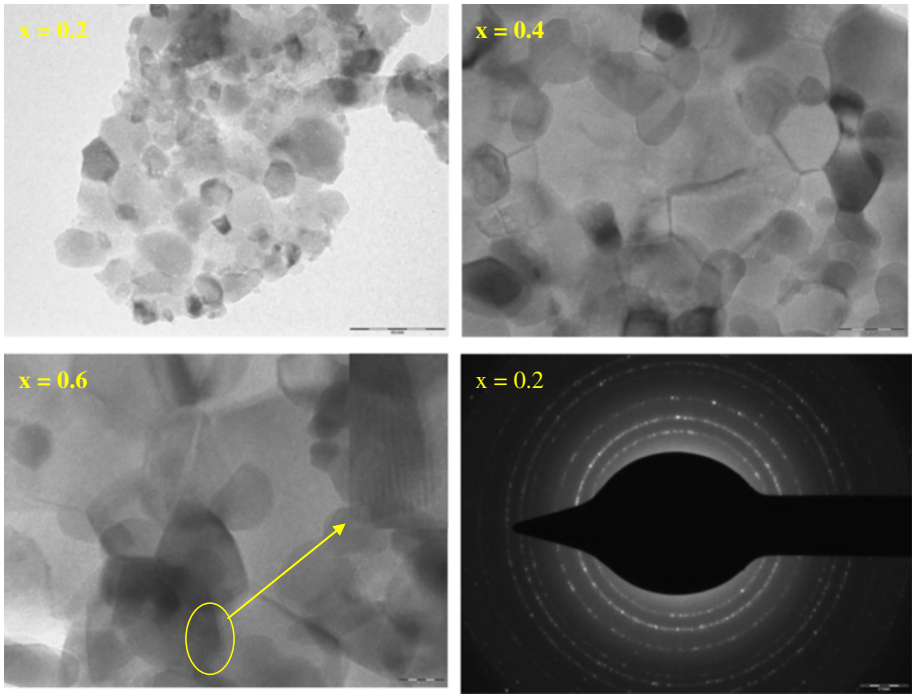

Figure 7 Transmission electron microscopy images of $Ni_{0.8-x}Zn_xCu_{0.2}Fe_2O_4$ (at 400°C).

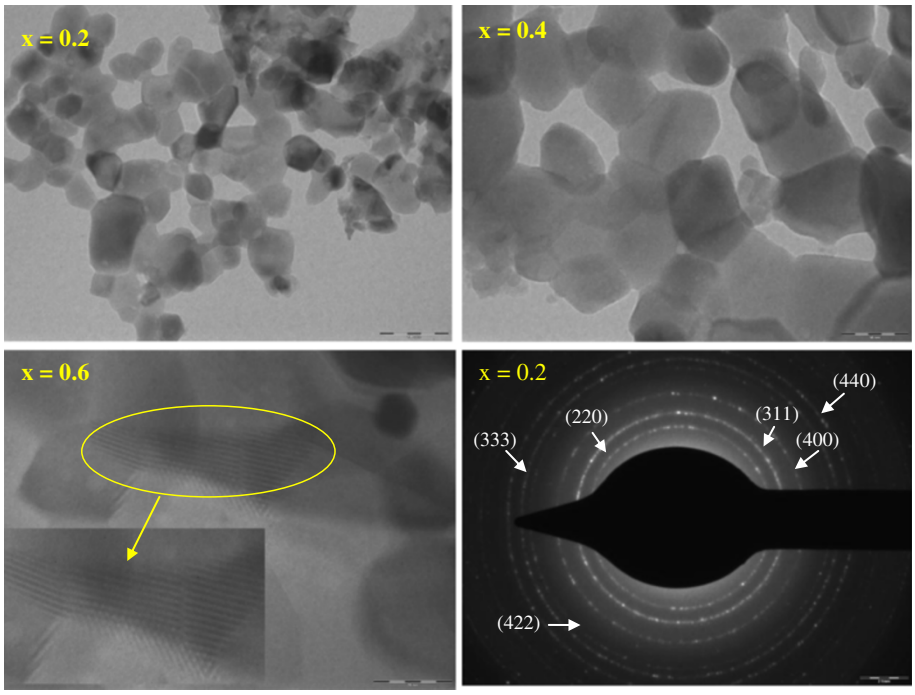

Figure 8 Transmission electron microscopy images of $Ni_{0.8-x}Zn_xCu_{0.2}Fe_2O_4$ (at 700°C).

sharp and intense. The weight loss that is about 3% at 400°C to 600°C is due to the dehydroxylation of the ferrite material, which occurs up to high temperatures, followed by the collapse of the pores and the densification of the nanoparticles.

Figure 3 represents the typical room-temperature powder X-ray diffraction patterns for the annealed samples (at 400°C and 700°C) which confirm the formation of a single-phase cubic spinel ferrite. The annealing treatment does not alter the crystal structure but increases the crystallinity of the samples. The lower peak intensity and broadening in XRD patterns show the nanocrystalline nature of the materials. The sintered samples show a sharp XRD peak indicating the increase in the crystalline nature of the samples. The average crystalline size of each composition is estimated from the XRD line width of the (311) diffraction peak using the Scherrer formulae ($D = 0.9\lambda/\beta\cos\theta$, where D is the crystallite diameter, λ is the radiation wavelength, and θ is the incidence angle) [21], and values are presented in Table 1. It is evident from Table 1 that an average homogeneous crystalline spinel phase enhances as the doping of Zn^{2+} ions and sintering temperature increases. The variation of the lattice constant with the composition (x) calculated using inter planner spacing (d) and Miller indices (hkl) is presented in Table 1.

Microstructural and chemical changes occurring in the system during heat treatment and Zn^{2+} substitutions are visible in Figures 4, 5, 6, 7, 8. The scanning electron microscope images of the samples obtained after heat treatment at 400°C and 700°C and presented in Figures 4 and 5 show the nanocrystalline nature, and crystallinity increases as the annealing temperature increases. This may be attributed to the fact that the growth of the crystal takes place in different orientations. The crystallographic images clearly indicate that the particles are stacked on top of each other because of their mutual magnetic interactions.

The TEM images together with the SAED pattern ($x = 0.2$) for representative compound results of $Ni_{0.8-x}Zn_xCu_{0.2}Fe_2O_4$ ($x = 0.2$, 0.4, and 0.6) nanoparticles are predicted in Figures 6, 7, 8. It has been observed that particles are aggregated during annealing and metal ion incorporation. The parallel lattice fringe is observed as uniformly extended over the primary building blocks, grain boundaries, and pores in the samples at $x = 0.6$ for all compositions, as shown in the insets of the said figures. Thus, it can be concluded that the nanoparticles are organized into an iso-oriented attached structure by sharing identical lattice planes.

The Fourier transform infrared spectra of the powder (as pellets in KBr) samples in the range 4,000 to 400 cm^{-1} were represented in Figure 9. The FTIR spectroscopy is a very useful technique to deduce not only the structural investigation and redistribution of cations between octahedral and tetrahedral sites of spinel ferrite nanoparticles, but also the lattice vibrational modes [22]. The FTIR spectra of all the samples exhibit two main

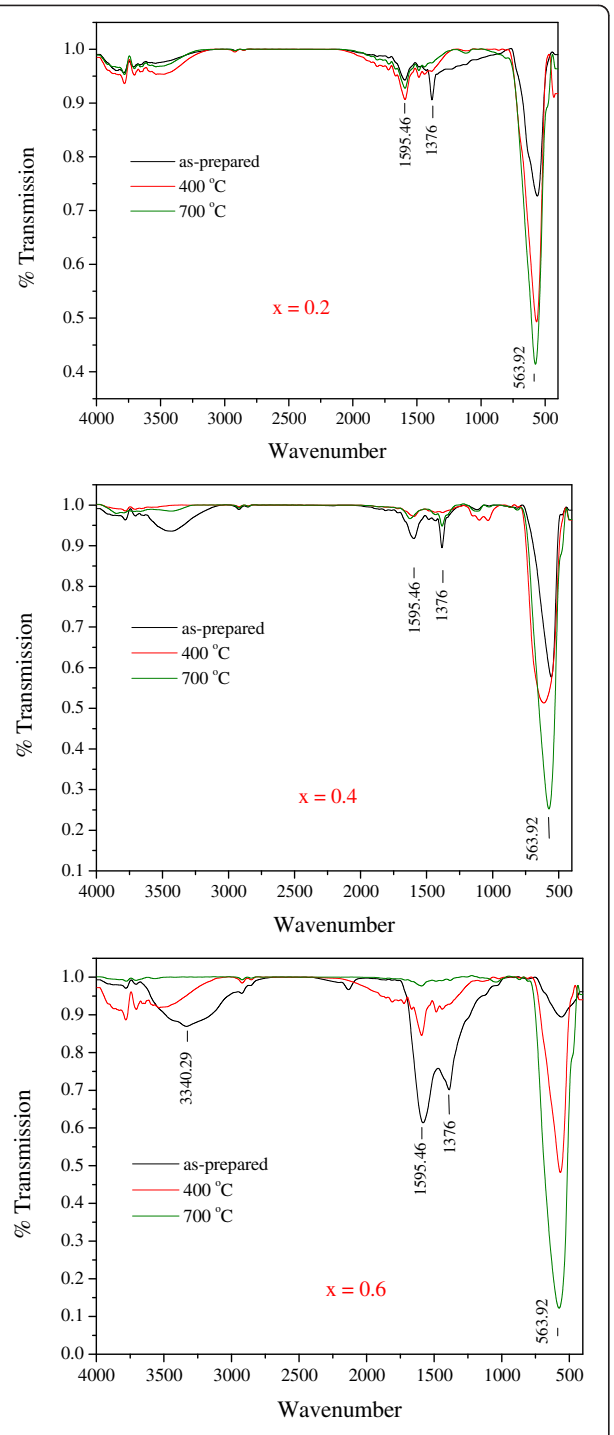

Figure 9 Fourier transform infrared spectra of $Ni_{0.8-x}Zn_xCu_{0.2}Fe_2O_4$.

absorption bands at wave numbers 600 and 400 cm^{-1} corresponding to intrinsic lattice vibrations of the ferrite skeleton for tetrahedral (A) and octahedral (B) sites, respectively [23]. The impurity peak is observed around 1,380 cm^{-1} in all the samples. The observed peak is attributed to the carboxyl group of C-O bonding. This may be due to the unreacted citric acid compound, which is used as fuel. The band around 1,600 cm^{-1} corresponds to the bending mode of H_2O molecules [24], and one more is observed at 3,100 to 3,450 cm^{-1} corresponding to hydrogen-bonded O-H groups [1]. During the combustion process, high temperature was generated. All carboxyl and hydroxyl groups appear with less intensity and disappear as the annealing temperature increases, confirming the single-phase nature of the sample as evident from the XRD results. The increase in the bandwidth and area of 564 cm^{-1} is attributed to the increase in crystallinity after the heat treatment; reverse observations are observed in SHI-irradiated nickel ferrite thin films by Dixit et al. [25]. The careful observation of FTIR data shows that the peak intensity at the octahedral site decreases as annealing temperature and Zn^{2+} contents increase showing that cations migrate from the octahedral (B) site to tetrahedral (A) site. This observation is also supporting the cation distribution obtained from the XRD results and exothermic peak observed at 370°C in DTA analysis.

Conclusions

The influence of Zn^{2+} doping in nanocrystalline Ni-Cu spinel ferrite was successfully studied by synthesizing the materials by the sol–gel auto-combustion technique and characterizing them using different tools. Thermal behavior of the as-prepared samples was confirmed by TG-DTA. The X-ray diffraction pattern reveals the formation of single-phase cubic spinel structure for all the compositions and temperatures. The crystallite size of the product was found in nanometric dimensions using a line profile fitting of the XRD pattern. The novel TEM morphological results with variations in the composition and sintering conditions are promising candidates for MLC technological applications. The chemical analysis and infrared spectral analysis of the prepared material confirm the formation of the spinel ferrite phase and the effect of preparation aids.

Competing interests

The authors declare that they have no competing interests.

Authors' contributions

VA, SR, MM, and KM have equal contributions. All authors read and approved the final manuscript.

Acknowledgments

VVA acknowledges financial support from BCUD, University of Pune and SAIF, IIT Mumbai for SEM, TEM facilities.

Author details

[1]Department of Physics, C. T. Bora College, Shirur, Pune 412210 (MS), India. [2]P.G.Department of Physics, Aabasaheb Garware College Pune (MS), Pune, India. [3]Department of Physics, S.G.R.G. Shinde Mahavidyalaya, Paranda 413502 (MS), India. [4]Department of Physics, H. V. Desai College, Pune (MS), India.

Received: 8 February 2013 Accepted: 1 April 2013
Published: 27 April 2013

References

1. Toksha, BG, Sagar, E, Shirsath, ML, Mane, SM, Patange, SS, Jadhav, SS, Jadhav, KM: Auto-combustion high-temperature synthesis, structural and magnetic properties of $CoCr_xFe_{2-x}O_4$ ($0 \le x \le 1.0$). J. Phys. Chem. C **115**, 20905 (2011)
2. Cannas, C, Ardu, A, Musinu, A, Peddis, D, Piccaluga, G: Spherical nanoporous assemblies of iso-oriented cobalt ferrite nanoparticles: synthesis, microstructure and magnetic properties. Chem. Mater. **20**, 6364 (2008)
3. Nandapure, AI, Kondawar, SB, Sawadh, PS, Nandapure, BI: Effect of zinc substitution on magnetic and electrical properties of nanocrystalline nickel ferrite synthesized by refluxing method. Physica. B. **407**, 1104 (2012)
4. Praveena, K, Sadhana, K, Murthy, SR: Elastic behaviour of microwave hydrothermally synthesized nanocrystalline Mn_{1-x}–Zn_x ferrites. Mater. Research Bulletin **47**, 1096 (2012)
5. Astruc, D, Lu, F, Aranzaes, JR: Nanoparticles as recyclable catalysts: the frontier between homogeneous and heterogeneous catalysis. Angew. Chem. Int. Ed. **44**, 7852 (2005)
6. Reetz, MT, Maase, M: Redox-controlled size-selective fabrication of nanostructured transition metal colloids. Adv. Mater. **11**, 773 (1999)
7. Rety, F, Clement, O, Siauve, N, Cuenod, CA, Carnot, F, Sich, M, Buisine, A, Frija, G: MR lymphography using iron oxide nanoparticles in rats: pharmacokinetics in the lymphatic system after intravenous injection. Magn. Reson. Imaging **12**, 734 (2000)
8. Rosensweig, R: Ferrohydrodynamics. Cambridge University Press, Cambridge, U.K. (1985)
9. Philip, J, Jaykumar, T, Sundaram, PK, Raj, B: A tunable optical filter. Meas. Sci. Technol. **14**, 1289 (2003)
10. Pankhurst, QA, Connolly, J, Jones, SK, Dobson, J: Applications of magnetic nanoparticles in biomedicine. J. Phys. D: Appl. Phys. **36**, R167 (2003)
11. Yavuz, CT, Mayo, JT, Yu, WW, Prakash, A, Falkner, JC, Yean, S, Cong, LL, Shipley, HJ, Kan, A, Tomson, M, Natelson, D, Colvin, VL: Low-Field Magnetic Separation of Monodisperse Fe3O4 Nanocrystals. Science **314**, 964 (2006)
12. Shirsath, SE, Kadam, RH, Patange, SM, Mane, ML, Ali, G, Akimitsu, M: Enhanced magnetic properties of Dy^{3+} substituted Ni-Cu-Zn ferrite nanoparticles. Appl. Phys. Lett. **100**, 042407 (2012)
13. Murbe, J, Topfer, J: High permeability Ni–Cu–Zn ferrites through additive-free low-temperature sintering of nanocrystalline powders. J. Europ. Ceramic Soc. **32**, 1091 (2012)
14. Li, Y, Zhao, J, Han, J, He, X: Combustion synthesis and characterization of NiCuZn ferrite powders. Mater. Research Bulletin **40**, 981 (2005)
15. Penchal Reddy, M, Balakrishnaiah, G, Madhuri, W, Venkata Ramana, M, Ramamanohar Reddy, N, Siva Kumar, KV, Murthy, VRK, Ramakrishna Reddy, R: Structural, magnetic and electrical properties of NiCuZn ferrites prepared by microwave sintering method suitable for MLCI applications. J. Phys. Chem. Solids **71**, 1373 (2010)
16. Raghavender, AT, Biliškov, N, Skoko, Ž: XRD and IR analysis of nanocrystalline Ni–Zn ferrite synthesized by the sol–gel method. Mater. Lett. **65**, 677 (2011)
17. Han, QJ, Ji, DH, Tang, GD, Li, ZZ, Hou, X, Qi, WH, Liu, SR, Bian, RR: Estimating the cation distributions in the spinel ferrites Cu0.5–xNi0.5ZnxFe2O4 ($0.0 \le x \le 0.5$). J. Magn. Magn. Mater **324**, 1975 (2012)
18. Jadhav, PA, Devan, RS, Kolekar, YD, Chougule, BK: Structural, electrical and magnetic characterizations of Ni–Cu–Zn ferrite synthesized by citrate precursor method. J. Phys. Chem. Solids **70**, 396 (2009)
19. Ghodake, SA, Ghodake, UR, Sawant, SR, Suryavanshi, SS, Bakare, PP: Magnetic properties of NiCuZn ferrites synthesized by oxalate precursor method. J. Magn. Magn. Mater. **305**, 110 (2006)
20. Murbe, J, Topfer, J: Low temperature sintering of sub-stoichiometric Ni–Cu–Zn ferrites: shrinkage, microstructure and permeability. J. Magn. Magn. Mater. **324**, 578 (2012)
21. Mane, ML, Dhage, VN, Sundar, R, Ranganathan, K, Oak, SM, Shengule, DR, Jadhav, KM: Effect of Nd: YAG laser irradiation on structural, morphological, cation distribution and magnetic properties of nanocrystalline $CoFe_2O_4$. Appl. Surf. Sci. **257**, 8511 (2011)
22. Prakash, I, Nallamuthu, N, Muralidharan, P, Venkateswarlu, M, Manjusri, M, Amar, M, Satyanarayana, N: Preparation and characterization of nanocrystalline CoFe2O4 deposited on SiO2: in situ sol–gel process. J. Sol–gel, Sci. Technol. **58**, 24 (2011)
23. Waldron, RD: Infrared spectra of ferrites. Phys. Rev. **99**, 1727 (1955)
24. Huang, Z, Zhu, Y, Wang, S, Yin, G: Controlled growth of aligned arrays of Cu–Ferrite nanorods. Cryst. Growth Des. **6**, 1931 (2006)
25. Dixit, G, Jitendra Pal, S, Srivastava, RC, Agrawal, HM: Study of 200 MeV Ag^{15+} ion induced amorphisation in nickel ferrite thin films. Nucl. Instrum. Methods B **269**, 133 (2011)

doi:10.1186/2228-5326-3-29
Cite this article as: Awati *et al.*: **Influence of Zn^{2+} doping on the structural and surface morphological properties of nanocrystalline Ni-Cu spinel ferrite.** *International Nano Letters* 2013 **3**:29.